

# Polynomial Chaos-Based Robust Design of Systems with Probabilistic Uncertainties

Dongying E. Shen and Richard D. Braatz

Dept. of Chemical Engineering, Massachusetts Institute of Technology, 77 Massachusetts Avenue, Cambridge, MA 02139

DOI 10.1002/aic.15373

Published online June 30, 2016 in Wiley Online Library (wileyonlinelibrary.com)

*A new algorithm is proposed for the design of nonlinear dynamical systems with probabilistic uncertainties. The dependence of the design objective and constraints on uncertainties is quantified by the polynomial chaos expansions (PCEs), while the relationships between the design parameters and the design objective/constraints are parameterized by Legendre polynomials. In two case studies, the polynomial chaos-based algorithm reduces the number of system evaluations required by optimization by an order of magnitude. Quantifying the dependence on uncertain parameters via the PCEs and including the quantification in design optimization simultaneously improved the distribution of the performance index and the probability of constraint fulfillment. © 2016 American Institute of Chemical Engineers AIChE J, 62: 3310–3318, 2016*

*Keywords:* design, design (batch plants), optimization, reactor analysis, statistical analysis

## Introduction

Models for real systems have associated uncertainties, which can influence the system performance and/or constraint satisfaction.<sup>1,2</sup> It is well established that ignoring uncertainties during design optimization can produce designs that are highly sensitive to uncertainties. The potential consequences of ignoring uncertainties during design include large variability in product quality<sup>3,4</sup> and higher total costs.<sup>5</sup>

Such studies have motivated the development of numerical algorithms that include uncertainties in optimal design problems. A popular strategy is to optimize designs based on a worst-case objective, which ensures that each system within an uncertainty set has the same or better objective than in worst case.<sup>6</sup> A design optimized for the worst-case uncertainty can result in poorer product quality or higher costs for more representative uncertainties than designs that do not consider the effects of uncertainties or that weigh more equally the effects of all uncertainties.<sup>7,8</sup> Worst-case design can be very conservative in practice, especially for systems in which the worst-case uncertainty has a vanishingly low probability of occurrence.

This article considers the optimal design of nonlinear dynamical systems with parametric uncertainties described by probability distribution functions (aka “probabilistic uncertainties”). For this type of uncertainty, the dominant strategy is to optimize the distribution of the objective and to satisfy constraints within specified probabilities. This strategy often requires estimation of the expected values and/or the variances of the objective and the constraints.<sup>3,9–12</sup> The Monte Carlo method, which samples

the probabilistic distributions and propagates these samples through the system models, is a common approach to estimate the expected values and the variances<sup>13</sup> but has a slow convergence rate on the order of  $1/\sqrt{n}$ , where  $n$  is the number of samples. As a result, the Monte Carlo method requires a large number of system simulations to accurately estimate the expected values and variances and is computationally expensive. More efficient sampling techniques, such as the Latin hypercube sampling<sup>14</sup> and the Hammersley sequence sampling,<sup>15</sup> have convergence rate on the order of  $1/n$ .

Another way to take uncertainties into account during design optimization is to employ Gaussian quadrature to estimate the integrals for the expected values and the variances.<sup>3,16</sup> These integrals are estimated each time that the optimizer accesses a new set of design inputs (the term “design inputs” is used instead of “design parameters” in the remainder of this article to avoid potential confusion with model parameters). Consequently, the number of system evaluations required by the optimal design calculations depends on the details of the optimizer and the closeness of the initial guess for the design inputs to the optimal solution.

Another method to account for uncertainties is via polynomial chaos theory, which uses polynomial expansions to approximate the dependence of system outputs on probabilistic uncertainties.<sup>17</sup> The polynomial expansions that achieve the fastest convergence rate have been derived for a wide variety of distributions (see Table 1), meaning that these expansions have the highest accuracy for expansions of the same order, and require the smallest number of terms to achieve a specified accuracy. With the optimal choices of polynomials in the table, the convergence rate is exponential and estimation of the means and variances is straightforward. Due to its low computational cost, the application of polynomial chaos to

Correspondence concerning this article should be addressed to R. D. Braatz at braatz@mit.edu.

**Table 1. Optimal Polynomial Expansions for Some Probabilistic Distributions<sup>17</sup>**

Uncertainty distributions $\boldsymbol{\eta}$	Optimal polynomial $\phi_i(\boldsymbol{\eta})$
Gaussian	Hermite
Uniform	Legendre
Gamma	Laguerre
Beta	Jacobi

chemical engineering and systems design problems has become of interest in recent years.<sup>4,8,9,18–21</sup>

This article proposes a new polynomial chaos-based algorithm for optimizing design inputs for systems with probabilistic uncertainties. To make the number of required system evaluations independent of the details of the optimizer and the initial guesses, this algorithm parameterizes the dependence of the optimization objective and constraints on design inputs with Legendre polynomials. In addition, the impacts of uncertainties on the objective and constraints are quantified by polynomial chaos expansions (PCEs) and included in the optimization. Computational efficiency of the design input parameterization and the robustness of polynomial chaos-based optimal designs are demonstrated in two case studies.

## Problem Statement

Consider a nonlinear dynamical system described by differential-algebraic equations:

$$\frac{d}{dt} \mathbf{x} = \mathbf{f}(t, \mathbf{x}, \mathbf{u}, \mathbf{k}, \boldsymbol{\eta}) \quad (1)$$

$$\mathbf{x}(t=0) = \mathbf{x}_0 \quad (2)$$

$$\mathbf{0} = \mathbf{z}(t, \mathbf{x}, \mathbf{u}, \mathbf{k}, \boldsymbol{\eta}), \quad (3)$$

for which  $t$  is time,  $\mathbf{x}$  is the vector of system states,  $\mathbf{u} \in \mathbb{R}^{n \times 1}$  is the vector of design inputs,  $\mathbf{k}$  is the vector of certain parameters (e.g., heat capacities),  $\boldsymbol{\eta}$  is the vector of parameters with probabilistic uncertainties,  $\mathbf{f}$  and  $\mathbf{z}$  are algebraic functions, and  $\mathbf{x}_0$  is the initial condition. The design inputs could include controller design parameters, initial conditions, and/or a parameterization of continuous-time trajectories such as temperature profiles. Although not explicitly treated here, the methodology described in this article can be directly extended to distributed parameter systems. To simplify the notation, the dependency on  $\mathbf{k}$  is suppressed in all functions subsequently defined in this article, but can be explicitly included without loss in generality.

The design optimization objective  $g$  and constraint function  $\mathbf{h} \in \mathbb{R}^{m \times 1}$  are functions of the design inputs and uncertain parameters,

$$g(\mathbf{u}, \boldsymbol{\eta}), \quad (4)$$

$$\mathbf{h}(\mathbf{u}, \boldsymbol{\eta}). \quad (5)$$

For example, a typical optimization objective for a batch design problem is

$$g(\mathbf{u}, \boldsymbol{\eta}) = \int_{t_0}^{t_f} \phi[\mathbf{x}(t)] dt + \zeta(t_f),$$

where  $t_0$  is the initial time,  $t_f$  is the final time, and  $\phi$  and  $\zeta$  are algebraic functions. Typical constraints are defined on the states evaluated at specific points in time or on integrals of the

states over time, with some examples given in the case studies.

With this nomenclature, the nominal optimal design problem is

$$\begin{aligned} & \min_{\mathbf{u} \in \mathcal{U}} g(\mathbf{u}, \boldsymbol{\eta}_{\text{nominal}}) \\ \text{s.t. } & \mathcal{U} = [\mathbf{u}_{1,\text{lower}}, \mathbf{u}_{1,\text{upper}}] \times \dots \times [\mathbf{u}_{n,\text{lower}}, \mathbf{u}_{n,\text{upper}}] \\ & \mathbf{h}(\mathbf{u}, \boldsymbol{\eta}_{\text{nominal}}) \leq \mathbf{0}. \end{aligned} \quad (6)$$

The design inputs are assumed to have known finite bounds. Typically such bounds can be specified using knowledge about the phenomena (e.g., that the mixing speed in a bioreactor must be less than some value to avoid cell damage) and/or thermodynamic and/or kinetic arguments (e.g., that the heat transfer system limits the temperature to be within some range). Solutions to this optimization can result in a wide distribution of the objective and/or a high probability of constraint violation in the presence of probabilistic uncertainties in  $\boldsymbol{\eta}$ . A well-known formulation of the design problem that reduces the effects of probabilistic uncertainties is

$$\begin{aligned} & \min_{\mathbf{u} \in \mathcal{U}} \mathbb{E}_{\boldsymbol{\eta}}[g(\mathbf{u}, \boldsymbol{\eta})] + \alpha_0 \text{Var}_{\boldsymbol{\eta}}[g(\mathbf{u}, \boldsymbol{\eta})] \\ \text{s.t. } & \mathcal{U} = [\mathbf{u}_{1,\text{lower}}, \mathbf{u}_{1,\text{upper}}] \times \dots \times [\mathbf{u}_{n,\text{lower}}, \mathbf{u}_{n,\text{upper}}] \\ & \mathbb{E}_{\boldsymbol{\eta}}[h_1(\mathbf{u}, \boldsymbol{\eta})] + \alpha_1 \text{Var}_{\boldsymbol{\eta}}[h_1(\mathbf{u}, \boldsymbol{\eta})] \leq 0 \\ & \mathbb{E}_{\boldsymbol{\eta}}[h_2(\mathbf{u}, \boldsymbol{\eta})] + \alpha_2 \text{Var}_{\boldsymbol{\eta}}[h_2(\mathbf{u}, \boldsymbol{\eta})] \leq 0 \\ & \vdots \\ & \mathbb{E}_{\boldsymbol{\eta}}[h_m(\mathbf{u}, \boldsymbol{\eta})] + \alpha_m \text{Var}_{\boldsymbol{\eta}}[h_m(\mathbf{u}, \boldsymbol{\eta})] \leq 0, \end{aligned} \quad (7)$$

where  $\mathbb{E}_{\boldsymbol{\eta}}$  and  $\text{Var}_{\boldsymbol{\eta}}$  are the expected value and the variance computed from integration with respect to  $\boldsymbol{\eta}$  and the set of scales  $\{\alpha_i\}$  control the tradeoffs between the expected values and the variances.\* This optimization requires inexpensive and accurate estimates for

1. the functional dependence of  $g(\mathbf{u}, \boldsymbol{\eta})$  and  $h_i(\mathbf{u}, \boldsymbol{\eta})$  on  $\boldsymbol{\eta}$  to quantify the effects of probabilistic uncertainties on the expected values and the variances;

2. the functional dependence of  $\mathbb{E}_{\boldsymbol{\eta}}[g(\mathbf{u}, \boldsymbol{\eta})]$ ,  $\text{Var}_{\boldsymbol{\eta}}[g(\mathbf{u}, \boldsymbol{\eta})]$ ,  $\mathbb{E}_{\boldsymbol{\eta}}[h_i(\mathbf{u}, \boldsymbol{\eta})]$ , and  $\text{Var}_{\boldsymbol{\eta}}[h_i(\mathbf{u}, \boldsymbol{\eta})]$  on the vector of design inputs  $\mathbf{u}$ .

## Proposed Approach

The first step of the approach is to approximate the dependence of the optimization objective and constraints on uncertainties with polynomial expansions:<sup>17</sup>

$$g(\mathbf{u}, \boldsymbol{\eta}) \approx \sum_{j=0}^{N_0} g_j(\mathbf{u}) \phi_j(\boldsymbol{\eta}),$$

$$h_i(\mathbf{u}, \boldsymbol{\eta}) \approx \sum_{j=0}^{N_i} h_{i,j}(\mathbf{u}) \phi_j(\boldsymbol{\eta}),$$

where the optimal polynomials  $\phi_j(\boldsymbol{\eta})$  depend on the distributions of  $\boldsymbol{\eta}$  and are given in Table 1, and the  $N_i$  are positive integers for all  $i$ . The polynomials in Table 1 have been proven to be optimal in terms of the  $L_2$  norm and have exponential convergence in the corresponding Hilbert functional space,<sup>17</sup> which results in accurate approximations even with a

\*For a design objective written as a maximization, the second term in (7) is multiplied by  $-1$ .

relatively small number of terms. The polynomials are orthogonal and satisfy

$$\langle \phi_i(\boldsymbol{\eta}), \phi_j(\boldsymbol{\eta}) \rangle = \int_{\mathbf{H}} \phi_i(\boldsymbol{\eta}) \phi_j(\boldsymbol{\eta}) d\mu(\boldsymbol{\eta}) = \begin{cases} \langle \phi_i^2(\boldsymbol{\eta}) \rangle & \text{if } i=j \\ 0 & \text{otherwise,} \end{cases} \quad (8)$$

where  $\mathbf{H}$  is the support for  $\boldsymbol{\eta}$  and  $\mu(\boldsymbol{\eta})$  is the weight function for  $\phi_i(\boldsymbol{\eta})$ . As a result of (8),

$$g_j(\mathbf{u}) = \frac{\langle g(\mathbf{u}, \boldsymbol{\eta}), \phi_j(\boldsymbol{\eta}) \rangle}{\langle \phi_j^2(\boldsymbol{\eta}) \rangle}. \quad (9)$$

Also, the expected value and the variance, which are computed from integration with respect to uncertainties, can be estimated once the expansion coefficients are computed:

$$\begin{aligned} \mathbb{E}_{\boldsymbol{\eta}}[g(\mathbf{u}, \boldsymbol{\eta})] &= \int_{\mathbf{H}} g(\mathbf{u}, \boldsymbol{\eta}) d\mu(\boldsymbol{\eta}) \\ &\approx \int_{\mathbf{H}} \sum_{j=0}^{N_0} g_j(\mathbf{u}) \phi_j(\boldsymbol{\eta}) d\mu(\boldsymbol{\eta}) \\ &= \sum_{j=0}^{N_0} g_j(\mathbf{u}) \int_{\mathbf{H}} \phi_j(\boldsymbol{\eta}) d\mu(\boldsymbol{\eta}) \end{aligned} \quad (10)$$

$$= \sum_{j=0}^{N_0} g_j(\mathbf{u}) \langle \phi_j(\boldsymbol{\eta}), 1 \rangle$$

$$= g_0(\mathbf{u}) \underbrace{\langle \phi_0(\boldsymbol{\eta}), 1 \rangle}_1$$

$$= g_0(\mathbf{u})$$

$$\begin{aligned} \text{Var}_{\boldsymbol{\eta}}[g(\mathbf{u}, \boldsymbol{\eta})] &= \mathbb{E}_{\boldsymbol{\eta}}[g^2(\mathbf{u}, \boldsymbol{\eta})] - \mathbb{E}_{\boldsymbol{\eta}}^2[g(\mathbf{u}, \boldsymbol{\eta})] \\ &= \int_{\mathbf{u}} g^2(\mathbf{u}, \boldsymbol{\eta}) d\mu(\boldsymbol{\eta}) - g_0^2(\mathbf{u}) \\ &\approx \sum_{j=0}^{N_0} g_j^2(\mathbf{u}) \langle \phi_j^2(\boldsymbol{\eta}) \rangle - g_0^2(\mathbf{u}) \\ &= \sum_{j=1}^{N_0} g_j^2(\mathbf{u}) \langle \phi_j^2(\boldsymbol{\eta}) \rangle. \end{aligned} \quad (11)$$

The above approach is described in several papers on polynomial chaos-based design.<sup>9</sup> For this approach, estimation of the expected values and the variances requires the computation of PCE coefficients. For simple systems, PCE coefficients can be computed via intrusive Galerkin projection, which takes the inner product of (1)–(3) with each basis function to obtain a system of equations for the expansion coefficients.<sup>17</sup> For more complex systems in which Galerkin projection cannot be applied, non-intrusive methods are used such as tensor-product quadrature, which estimates the integral for the numerator of (9), and linear regression, which solves for the complete set of expansion coefficients by evaluating the original system for selected values for uncertainties.<sup>22</sup>

A drawback of using (10) and (11) in (7) is that the expansion coefficients  $g_j(\mathbf{u})$  and  $h_{i,j}(\mathbf{u})$  would need to be evaluated for every new  $\mathbf{u}$  that the optimizer accesses. Since the evaluation of the expansion coefficients requires system evaluations (i.e., simulations of (1)–(3)), the computational cost of the

optimization is influenced by the choice of initial guesses and the effectiveness of the optimizer for the particular optimization. We propose to resolve this issue by approximating the dependence of the objective and constraints on the design inputs by their approximation by an expansion of Legendre polynomials:

$$g(\mathbf{u}, \boldsymbol{\eta}) \approx \sum_{j=0}^{n_0} \sum_{k=0}^{m_0} g_{jk} \phi_j(\boldsymbol{\eta}) P_k(\mathbf{u}) \quad (12)$$

$$h_i(\mathbf{u}, \boldsymbol{\eta}) \approx \sum_{j=0}^{n_i} \sum_{k=0}^{m_i} h_{ijk} \phi_j(\boldsymbol{\eta}) P_k(\mathbf{u}), \quad (13)$$

where  $P_k(\mathbf{u})$  is the Legendre polynomial in  $\mathbf{u}$  of degree  $k$ , and  $n_i$  and  $m_i$  are positive integers for all  $i$ . These equations are referred to as *design input parameterization* in this article.

In (12) and (13), the dependence of the expected values and the variances on the design inputs can be cheaply computed from the expansion coefficients  $g_{jk}$  and  $h_{ijk}$  and the relations

$$\begin{aligned} \mathbb{E}_{\boldsymbol{\eta}}[g(\mathbf{u}, \boldsymbol{\eta})] &= \int_{\mathbf{H}} g(\mathbf{u}, \boldsymbol{\eta}) d\mu(\boldsymbol{\eta}) \\ &\approx \sum_{j=0}^{n_0} \sum_{k=0}^{m_0} g_{jk} P_k(\mathbf{u}) \int_{\mathbf{H}} \phi_j(\boldsymbol{\eta}) d\mu(\boldsymbol{\eta}) \end{aligned} \quad (14)$$

$$\approx \sum_{j=0}^{n_0} \sum_{k=0}^{m_0} g_{jk} P_k(\mathbf{u}) \langle \phi_j(\boldsymbol{\eta}) \rangle$$

$$\begin{aligned} \text{Var}_{\boldsymbol{\eta}}[g(\mathbf{u}, \boldsymbol{\eta})] &= \mathbb{E}_{\boldsymbol{\eta}}[g^2(\mathbf{u}, \boldsymbol{\eta})] - \mathbb{E}_{\boldsymbol{\eta}}^2[g(\mathbf{u}, \boldsymbol{\eta})] \\ &\approx \int_{\mathbf{H}} \left[ \sum_{j=0}^{n_0} \sum_{k=0}^{m_0} g_{jk} \phi_j(\boldsymbol{\eta}) P_k(\mathbf{u}) \right]^2 d\mu(\boldsymbol{\eta}) - \left[ \sum_{j=0}^{n_0} \sum_{k=0}^{m_0} g_{jk} P_k(\mathbf{u}) \langle \phi_j(\boldsymbol{\eta}) \rangle \right]^2. \end{aligned} \quad (15)$$

The novelty of the proposed representation of the design inputs is the one-time evaluation of the expansion coefficients  $g_{jk}$  and  $h_{ijk}$  before (14) and (15) are sent to the optimizer. The other novelty of the polynomial dependence of the expected values and the variances on the design inputs in (14) and (15) is the polynomial dependence of the optimization objective and constraints. Therefore, the computational cost of the optimization, which mainly depends on the number of system evaluations, is fixed. In summary, the proposed approach for designing systems with probabilistic uncertainties consists of three steps:

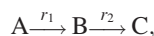
1. compute the expansion coefficients  $g_{jk}$  and  $h_{ijk}$ ;
2. express the expected values and the variances of the optimization objective and constraints as polynomial functions of the design inputs using (14) and (15);
3. send these functions to the optimizer to find the optimal design inputs.

## Case Studies

This section applies the proposed approach to two chemical reactor design problems. Tensor-product quadrature was used to determine the PCE coefficients.<sup>22</sup> All optimizations were solved using `fmincon` of MATLAB<sup>®</sup>.

## Optimal design of a batch chemical reactor with series reactions

Consider the chemical reactions in series,



in a batch reactor where

$$r_1 = k_{10} \exp\left(-\frac{E_1}{RT}\right) C_A,$$

$$r_2 = k_{20} \exp\left(-\frac{E_2}{RT}\right) C_B,$$

$R$  is the gas constant,  $T$  is the reaction temperature,  $E_i$  are activation energies,  $k_{i0}$  are prefactors, and the reaction parameters are listed in Table 2. The design objective is to find the reaction temperature  $T$  that maximizes the concentration of the desired intermediate product B, which is produced from species A but consumed by the chemical reaction that converts species B to species C. The nominal optimization of reaction temperature, which does not consider the dependence of  $C_B(t_f, k_{10}, k_{20}, T)$  on the uncertainties in the prefactors  $k_{10}$  and  $k_{20}$ , is

$$\max_{300\text{K} \leq T \leq 400\text{K}} C_B(t_f, k_{10,\text{nominal}}, k_{20,\text{nominal}}, T).$$

The nominal optimal temperature  $T$  is 324.69 K, which produces a maximum  $C_B(t_f, k_{10,\text{nominal}}, k_{20,\text{nominal}}, T)$  of 199.06 M.

The uniformly distributed uncertainties in the prefactors  $k_{10}$  and  $k_{20}$  in Table 2 result in a distribution in the intermediate concentration  $C_B(t_f, k_{10}, k_{20}, T)$ . The optimal design problem that takes the probabilistic uncertainties into account is

$$\max_{300\text{K} \leq T \leq 400\text{K}} \{E_{k_{10}, k_{20}}[C_B(t_f, k_{10}, k_{20}, T)] - \alpha \text{Var}_{k_{10}, k_{20}}[C_B(t_f, k_{10}, k_{20}, T)]\}, \quad (16)$$

where  $\alpha$  quantifies the tradeoff between the maximization of the expected value and the reduction of the variance.

The dependence of the final intermediate concentration  $C_B(t_f, k_{10}, k_{20}, T)$  on the uncertain prefactors  $k_{10}$  and  $k_{20}$  is quantified via PCEs, and the dependence on  $T$  is parameterized by Legendre polynomials:

$$\begin{aligned} C_B(t_f, k_{10}, k_{20}, T) &\approx \sum_{n=0}^N C_{Bn}(t_f) \phi_n(k_{10}, k_{20}, T) \\ &= \sum_{n=0}^N C_{Bn}(t_f) \phi_n(k'_{10}, k'_{20}, T'), \end{aligned}$$

where

**Table 2. Parameters for the Batch Reactor Case Study**

$k_{10}$ ( $\text{s}^{-1}$ )	Uniformly distributed between 100 and 1000; nominal value at 550
$E_1/R$ (K)	2400
$k_{20}$ ( $\text{s}^{-1}$ )	Uniformly distributed between 100 and 1000; nominal value at 550
$E_2/R$ (K)	4800
Reaction time $t_f$ (s)	20
Reaction temperature $T$ (K)	Between 300 and 400
Initial $C_A$ (M)	200
Initial $C_B$ (M)	0
Initial $C_C$ (M)	0

$$k'_{10} = \frac{k_{10} - k_{10,m}}{k_{10,d}} \sim \mathcal{U}(-1, 1)$$

$$k_{10,m} = \frac{k_{10,\text{upper bound}} + k_{10,\text{lower bound}}}{2}$$

$$k_{10,d} = \frac{k_{10,\text{upper bound}} - k_{10,\text{lower bound}}}{2}$$

$$k'_{20} = \frac{k_{20} - k_{20,m}}{k_{20,d}} \sim \mathcal{U}(-1, 1)$$

$$k_{20,m} = \frac{k_{20,\text{upper bound}} + k_{20,\text{lower bound}}}{2}$$

$$k_{20,d} = \frac{k_{20,\text{upper bound}} - k_{20,\text{lower bound}}}{2}$$

$$T' = \frac{T - T_m}{T_d} \sim \mathcal{U}(-1, 1)$$

$$T_m = \frac{T_{\text{upper bound}} + T_{\text{lower bound}}}{2}$$

$$T_d = \frac{T_{\text{upper bound}} - T_{\text{lower bound}}}{2}$$

$N$  is the total number of basis functions used in the expansion, and  $\phi_n(k'_{10}, k'_{20}, T')$  is the  $n^{\text{th}}$  basis function, which is the product of the Legendre polynomials in  $k'_{10}$ ,  $k'_{20}$ , and  $T'$ .

The evaluation of the expansion coefficients  $C_{Bn}(t_f)$  uses (8):

$$\begin{aligned} \langle C_B(t_f, k_{10}, k_{20}, T), \phi_n(k'_{10}, k'_{20}, T') \rangle &= C_{Bn}(t_f) \langle \phi_n^2(k'_{10}, k'_{20}, T') \rangle \\ C_{Bn}(t_f) &= \frac{\langle C_B(t_f, k_{10}, k_{20}, T), \phi_n(k'_{10}, k'_{20}, T') \rangle}{\langle \phi_n^2(k'_{10}, k'_{20}, T') \rangle}, \end{aligned}$$

where the numerator is

$$\int_{-1}^1 \int_{-1}^1 \int_{-1}^1 C_B(t_f, k_{10}, k_{20}, T) \phi_n(k'_{10}, k'_{20}, T') w(k'_{10}, k'_{20}, T') dk'_{10} dk'_{20} dT', \quad (17)$$

and the denominator is

$$\int_{-1}^1 \int_{-1}^1 \int_{-1}^1 \phi_n^2(k'_{10}, k'_{20}, T') w(k'_{10}, k'_{20}, T') dk'_{10} dk'_{20} dT', \quad (18)$$

where

$$w(k'_{10}, k'_{20}, T') = \left(\frac{1}{2}\right)^3 = \frac{1}{8}. \quad (19)$$

**Table 3. The Highest Degrees of the Legendre Polynomials in  $k'_{10}$ ,  $k'_{20}$ , and  $T'$  and the Number of the Gauss-Legendre Quadrature Points Used to Approximate the Integral in (17) for the Batch Reactor Case Study**

Highest degree of the Legendre polynomials in $k'_{10}$ and $k'_{20}$	5
$I$ and $J$	6
Highest degree of the Legendre polynomials in $T'$	2
$K$	3
Number of system evaluations for computing PCE coefficients for a new $T$ without design input parameterization	$6^2 = 36$
Number of system evaluations for computing PCE coefficients with design input parameterization	$6^2 \times 3 = 108$

Equation 18 is the inner product of the square of the  $n^{\text{th}}$  basis function, and therefore depends on only the distributions of the uncertain parameters. Conversely, the integral in (17) can be approximated by Gaussian-Legendre quadrature, which evaluates  $C_B(t_f, k_{10}, k_{20}, T)$  for different values of  $k_{10}$ ,  $k_{20}$ , and  $T$ :

$$(17) \approx \sum_{i=1}^I \sum_{j=1}^J \sum_{k=1}^K C_B(t_f, \bar{k}_{10,i}, \bar{k}_{20,j}, \bar{T}_k) \phi_n(\bar{k}_{10,i}, \bar{k}_{20,j}, \bar{T}_k) w(\bar{k}_{10,i}) w(\bar{k}_{20,j}) w(\bar{T}_k),$$

where

$\bar{k}_{10,i}$  = the  $i^{\text{th}}$  root of  $P_I$ , the Legendre polynomial of degree  $I$

$$w(\bar{k}_{10,i}) = \frac{1}{(1 - \bar{k}_{10,i}^2) [P'_I(\bar{k}_{10,i})]^2}$$

$P'_I(\bar{k}_{10,i})$  = the derivative of  $P_I$  evaluated at  $\bar{k}_{10,i}$

$\bar{k}_{20,j}$  = the  $j^{\text{th}}$  root of  $P_J$ , the Legendre polynomial of degree  $J$

$$w(\bar{k}_{20,j}) = \frac{1}{(1 - \bar{k}_{20,j}^2) [P'_J(\bar{k}_{20,j})]^2}$$

$P'_J(\bar{k}_{20,j})$  = the derivative of  $P_J$  evaluated at  $\bar{k}_{20,j}$

$\bar{T}_k$  = the  $k^{\text{th}}$  root of  $P_K$ , the Legendre polynomial of degree  $K$

$$w(\bar{T}_k) = \frac{1}{(1 - \bar{T}_k^2) [P'_K(\bar{T}_k)]^2}$$

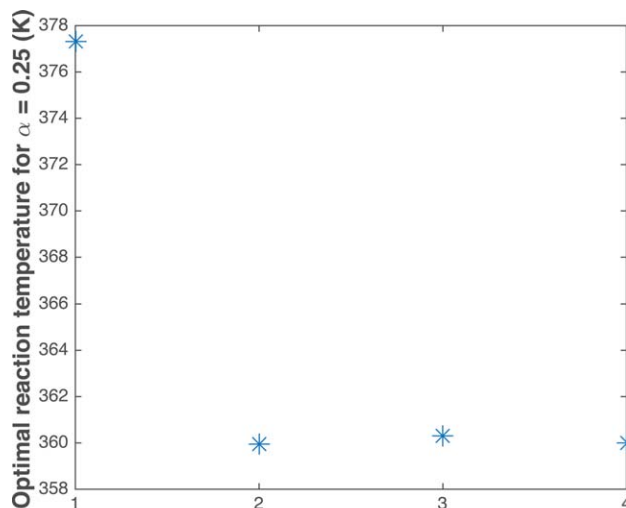
$P'_K(\bar{T}_k)$  = the derivative of  $P_K$  evaluated at  $\bar{T}_k$

$C_B(t_f, \bar{k}_{10,i}, \bar{k}_{20,j}, \bar{T}_k) = C_B(t_f)$  evaluated at  $\bar{k}_{10,i}$ ,  $\bar{k}_{20,j}$ , and  $\bar{T}_k$

$\phi_n(\bar{k}_{10,i}, \bar{k}_{20,j}, \bar{T}_k) = \phi_n$  evaluated at  $\bar{k}_{10,i}$ ,  $\bar{k}_{20,j}$ , and  $\bar{T}_k$

and  $I, J, K$  are positive integers. Table 3 lists the highest degrees of the Legendre polynomials in  $k'_{10}$ ,  $k'_{20}$ , and  $T'$  and the values for  $I, J, K$ . For a PCE of order  $p$ , the minimum order of Gaussian quadrature to obtain accurate computation of all of the PCE coefficients is  $p + 1$ .<sup>22</sup> As additional points would require more computational cost, the minimum order of Gaussian quadrature of  $p + 1$  was used in both case studies. Figure 1 shows that choosing the highest degree of the Legendre polynomial in  $T'$  as two produced low approximation error. Once the expansion coefficients  $C_{Bn}(t_f)$  are evaluated,  $\mathbb{E}_{k_{10}, k_{20}}[C_B(t_f, k_{10}, k_{20}, T)]$ ,  $\text{Var}_{k_{10}, k_{20}}[C_B(t_f, k_{10}, k_{20}, T)]$ , and therefore the objective in (16) are approximated by polynomial functions in  $T'$ .

A pareto-optimality plot is a commonly used approach for the selection of values for parameters that trade off multiple objectives. Figure 2 shows the pareto-optimality plot of the expected values and the variances of the intermediate concentration  $C_B(t_f, k_{10}, k_{20}, T)$  at the optimal temperature for different values for  $\alpha$  in the optimal design problem. The reaction temperature of 359.71 K corresponds to a value of  $\alpha$  of 0.25, which is located approximately at the knee of the curve. The 35.02 K difference between the optimal temperature for the nominal values of the prefactor  $k_{10}$  and  $k_{20}$  and that from the polynomial chaos-based optimization results in drastically different distributions of  $C_B(t_f, k_{10}, k_{20}, T)$  (see Figure 3 and Table 4). Specifically, the distribution of  $C_B(t_f, k_{10}, k_{20}, T)$  for the polynomial chaos-based optimal temperature has a higher average and a much smaller standard deviation than for the



Highest degree of the Legendre polynomial in  $T'$

**Figure 1.** The convergence plot for the batch reactor case study: the highest degree of the Legendre polynomials in  $T'$  was based on the convergence of the optimal temperature for  $\alpha = 0.25$ .

[Color figure can be viewed in the online issue, which is available at [wileyonlinelibrary.com](http://wileyonlinelibrary.com).]

optimal temperature for the nominal values of  $k_{10}$  and  $k_{20}$ . This difference demonstrates the importance of including the effects of parametric uncertainties in optimal design problems.

The effect of design input parameterization on computational cost was also examined. When a PCE without design input parameterization,

$$C_B(t_f, k_{10}, k_{20}, T) \approx \sum_{n=0}^M C_{Bn}(t_f, T) \phi_n(k_{10}, k_{20}),$$

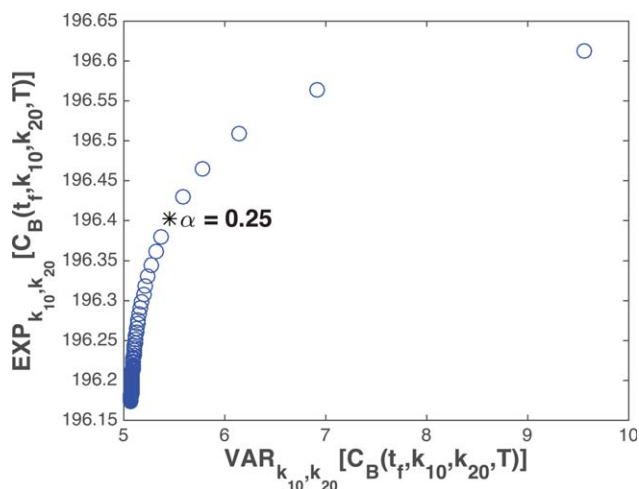


**Figure 2.** The pareto-optimality plot for the batch reactor case study that shows how  $\mathbb{E}_{k_{10}, k_{20}}[C_B(t_f, k_{10}, k_{20}, T)]$  changes with  $\text{Var}_{k_{10}, k_{20}}[C_B(t_f, k_{10}, k_{20}, T)]$ .

A value of  $\alpha$  of 0.25 is located at the knee of the curve.

[Color figure can be viewed in the online issue, which is available at [wileyonlinelibrary.com](http://wileyonlinelibrary.com).]

was used to approximate the dependence of the intermediate concentration  $C_B(t_f, k_{10}, k_{20}, T)$  on the uncertain parameters, the expansion coefficients  $C_{Bn}(t_f, T)$  were evaluated for every new temperature the optimizer accessed. With the computed expansion coefficients,  $\mathbb{E}_{k_{10}, k_{20}}[C_B(t_f, k_{10}, k_{20}, T)]$  and  $\text{Var}_{k_{10}, k_{20}}[C_B(t_f, k_{10}, k_{20}, T)]$  were computed from

$$\begin{aligned} \mathbb{E}_{k_{10}, k_{20}}[C_B(t_f, k_{10}, k_{20}, T)] &\approx \left\langle \sum_{n=0}^M C_{Bn}(t_f, T) \phi_n(k_{10}, k_{20}), 1 \right\rangle \\ &= C_{B0}(t_f, T); \\ \text{Var}_{k_{10}, k_{20}}[C_B(t_f, k_{10}, k_{20}, T)] &= \mathbb{E}_{k_{10}, k_{20}}[C_B^2(t_f, k_{10}, k_{20}, T)] \\ &\quad - (\mathbb{E}_{k_{10}, k_{20}}[C_B(t_f, k_{10}, k_{20}, T)])^2 \\ &\approx \left\langle \sum_{n=0}^M C_{Bn}(t_f, T) \phi_n(k_{10}, k_{20}), \sum_{n=0}^M C_{Bn}(t_f, T) \phi_n(k_{10}, k_{20}) \right\rangle \\ &\quad - C_{B0}^2(t_f, T) \\ &= \sum_{n=0}^M C_{Bn}^2(t_f, T) \langle \phi_n^2(k_{10}, k_{20}) \rangle - C_{B0}^2(t_f, T) \\ &= \sum_{n=1}^M C_{Bn}^2(t_f, T) \langle \phi_n^2(k_{10}, k_{20}) \rangle. \end{aligned}$$

When `fmincon` of MATLAB<sup>®</sup> was used to find the reaction temperature that maximizes  $\mathbb{E}_{k_{10}, k_{20}}[C_B(t_f, k_{10}, k_{20}, T)] - 0.25 \text{Var}_{k_{10}, k_{20}}[C_B(t_f, k_{10}, k_{20}, T)]$ , the number of system evaluations without design input parameterization was 576, whereas that with design input parameterization was 108. The design input parameterization reduced computational cost by about a factor of 5.

### Optimal design of a tubular reactor with a five-species reaction network

Molar balances for the five species in the reaction network in Figure 5 carried out in a microscale automated continuous-flow tubular reactor are<sup>23</sup>

$$\begin{aligned} \frac{dC_1}{dt} &= -k_1 C_1 C_2 - k_2 C_1 C_2 \\ \frac{dC_2}{dt} &= -k_1 C_1 C_2 - k_2 C_1 C_2 - k_3 C_2 C_3 - k_4 C_2 C_4 \\ \frac{dC_3}{dt} &= k_1 C_1 C_2 - k_3 C_2 C_3 \\ \frac{dC_4}{dt} &= k_2 C_1 C_2 - k_4 C_2 C_4 \\ \frac{dC_5}{dt} &= k_3 C_2 C_3 + k_4 C_2 C_4, \end{aligned}$$

where

$$k_i = A_i \exp\left(-\frac{E_{Ai}}{RT}\right),$$

$t$  is the distance down the reactor multiplied by its cross-sectional area and divided by the volumetric flow rate of the feed stream, and the reaction parameters are listed in Table 5. The nominal reactor design problem is to determine the residence time that maximizes the concentration of the intermediate compound 4 while limiting reactant to be at most 1% of its feed concentration:

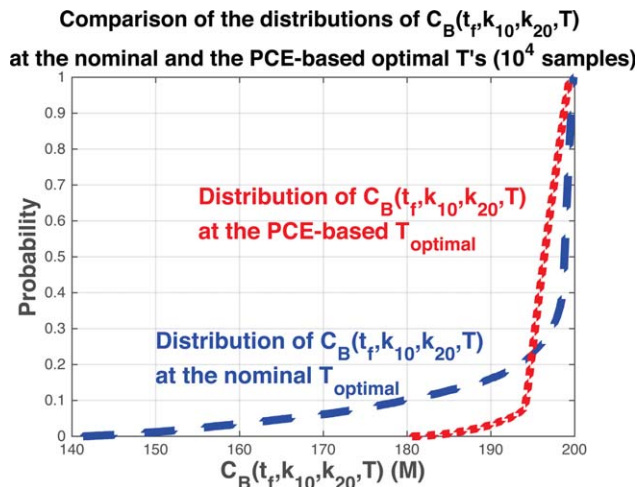


**Figure 3.** Comparison of the distributions of the intermediate concentration  $C_B(t_f, k_{10}, k_{20}, T)$  at the nominal and polynomial chaos-based optimal temperatures for the batch reactor case study constructed from  $10^4$  Monte Carlo simulation samples.

[Color figure can be viewed in the online issue, which is available at [wileyonlinelibrary.com](http://wileyonlinelibrary.com).]

$$\begin{aligned} \max_{0.5 \text{ min} \leq t_{\text{res}} \leq 20 \text{ min}} & \frac{C_4(\log_{10} A_1, \log_{10} A_4, t_{\text{res}})}{C_{10}} \\ \text{s.t.} & \frac{C_1(\log_{10} A_1, \log_{10} A_4, t_{\text{res}})}{C_{10}} \leq 1\%. \end{aligned}$$

The solution is the optimal residence time for the tubular reactor, which is 0.921 min.

The uncertainties in  $\log_{10} A_1$  and  $\log_{10} A_4$  lead to distributions of  $C_1(\log_{10} A_1, \log_{10} A_4, t_{\text{res}})$  and  $C_4(\log_{10} A_1, \log_{10} A_4, t_{\text{res}})$ , which are taken into account in the reactor design problem as

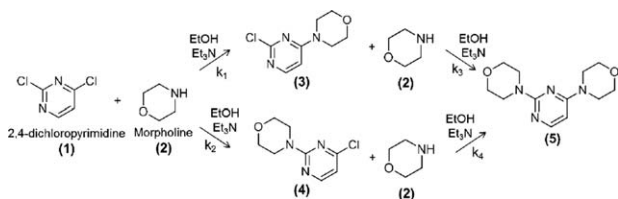
$$\begin{aligned} \max_{0.5 \text{ min} \leq t_{\text{res}} \leq 20 \text{ min}} & \left\{ \mathbb{E}_{\log_{10} A_1, \log_{10} A_4} \left[ \frac{C_4(\log_{10} A_1, \log_{10} A_4, t_{\text{res}})}{C_{10}} \right] \right. \\ & \left. - \alpha \text{Var}_{\log_{10} A_1, \log_{10} A_4} \left[ \frac{C_4(\log_{10} A_1, \log_{10} A_4, t_{\text{res}})}{C_{10}} \right] \right\} \\ \text{s.t.} & \mathbb{E}_{\log_{10} A_1, \log_{10} A_4} \left[ \frac{C_1(\log_{10} A_1, \log_{10} A_4, t_{\text{res}})}{C_{10}} \right] \leq 1\%. \end{aligned}$$

Table 6 lists the highest degrees of the Legendre polynomials used for approximating the dependence of the concentrations  $C_1$  and  $C_4$  on  $\log_{10} A_1$ ,  $\log_{10} A_4$ , and  $t_{\text{res}}$  and the number of Gauss-Legendre quadrature points used to compute the expansion coefficients.

The pareto-optimality curve for the expected values and the variances of the intermediate concentration  $C_4(\log_{10} A_1, \log_{10}$

**Table 4.** Averages and Standard Deviations of  $10^4$  Samples for the Nominal and the Polynomial Chaos-Based Optimal Temperatures for the Batch Reactor Case Study

Optimization	Temperature (K)	Average (M)	Standard deviation (M)
Nominal	324.69	194.12	11.03
PCE	359.96	196.17	2.51



**Figure 4. Chemical reaction network for the tubular reactor.**<sup>23</sup>

**Table 5. Parameters for the Tubular Reactor Case Study**<sup>23</sup>

$C_{10}$ (M)	0.150
$C_{20}$ (M)	0.375
$T$ (K)	373.15
$t_{res}$ (min)	Between 0.5 and 20
$R$ (J/mol·K)	8.314
$\log_{10} A_1; A_i$ ( $M^{-1}s^{-1}$ )	uniformly distributed within [3.0, 3.8]; nominal value at 3.4
$E_{A1}$ (kJ/mol)	27
$\log_{10} A_2$	3.5
$E_{A2}$ (kJ/mol)	32.1
$\log_{10} A_3$	4.9
$E_{A3}$ (kJ/mol)	60.0
$\log_{10} A_4$	Uniformly distributed within [2.6, 3.4]; nominal value at 3.0
$E_{A4}$ (kJ/mol)	45

$A_4, t_{res}$ ) at optimal residence times for different values of  $\alpha$  is shown in Figure 5. A value of  $\alpha$  of 115 was selected as a reasonable tradeoff between the expected value and the variance, which has the corresponding optimal residence time of 8.320 min. Figures 6 and 7 show that the polynomial chaos-based optimal residence time has 100% constraint satisfaction for  $\frac{C_1}{C_{10}}$  without significantly reducing the maximum intermediate concentration  $\frac{C_4}{C_{10}}$ , whereas there is approximately 18% chance of constraint violation for the optimal residence time for the nominal values of  $\log_{10} A_1$  and  $\log_{10} A_4$ .

The effect of design input parameterization on computational cost was also examined. The number of system evaluations without parameterization of  $t_{res}$  was 2100, and was 125 with parameterization of  $t_{res}$ , representing a reduction of more than one order of magnitude in computational cost.

In general, the relative computational cost of using design-input parameterization vs. not using design-input parameterization depends on the order of the PCE with respect to the design input. The optimization approach without design-input parameterization using the Legendre polynomials will require fewer evaluations if a very high order of the PCE with respect to the design input is needed to accurately approximate the relationship between the design input and the robust optimization objective.

Both case studies had uniformly distributed uncertain parameters. Replacing the uniform distributions with other types of distributions would involve replacing the Legendre

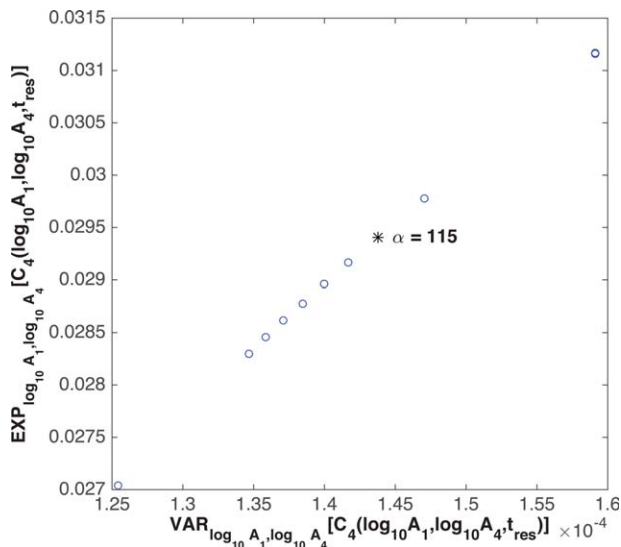


**Figure 5. The pareto-optimality plot for the tubular reactor case study showing the tradeoff between  $E_{\log_{10} A_1, \log_{10} A_4} [C_4(\log_{10} A_1, \log_{10} A_4, t_{res})]$  and  $Var_{\log_{10} A_1, \log_{10} A_4} [C_4(\log_{10} A_1, \log_{10} A_4, t_{res})]$  for different values of  $\alpha$ .**

[Color figure can be viewed in the online issue, which is available at [wileyonlinelibrary.com](http://wileyonlinelibrary.com).]

polynomials for the uncertain parameters with other polynomials as shown in Table 1. As in the case studies that had uniformly distributed uncertain parameters, the computational cost would be a function of the order of the PCEs.

## Conclusions

This article proposes a polynomial chaos-based approach for the design of nonlinear dynamical systems with probabilistic uncertainties and bounds on the design inputs. The two characteristics of this design approach are

1. the dependence of the optimization objective and constraints on design inputs is parameterized with Legendre polynomials, and
2. the effects of the uncertainties on the objective and constraints are quantified by PCEs.

The designs of batch and continuous-flow chemical reactors were optimized with this method in the presence of uniformly distributed uncertain parameters.

For a batch reactor with series reactions, the reaction temperature was optimized to maximize the concentration of a desired intermediate species in the presence of two uncertain kinetic parameters. Compared to the optimal reaction temperature from the nominal optimization, the polynomial chaos-based optimal temperature produced a distribution of the

**Table 6. The Highest Degrees of the Legendre Polynomials in  $\log_{10} A_1$ ,  $\log_{10} A_4$ , and  $t_{res}$  and the Number of the Gauss-Legendre Quadrature Points Used to Approximate the Expansion Coefficients for the Tubular Reactor Case Study**

Highest degree of the Legendre polynomials in $\log_{10} A_1$ and $\log_{10} A_4$	4
Number of quadrature points for each uncertain parameter	5
Highest degree of the Legendre polynomials in $t_{res}$	4
Number of quadrature points for $t_{res}$	5
Number of system evaluations for computing PCE coefficients for a new $t_{res}$ without design input parameterization	$5^2 = 25$
Number of system evaluations for computing PCE coefficients with design input parameterization	$5^2 \times 5 = 125$

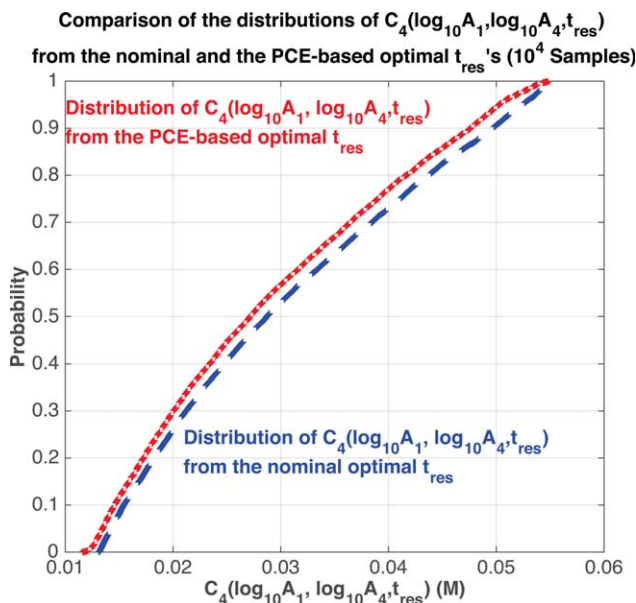


**Figure 6.** Comparison of the probability distribution functions of the intermediate concentration  $C_4(\log_{10} A_1, \log_{10} A_4, t_{res})$  from the nominal and the polynomial chaos-based optimal residence times for the tubular reactor case study, constructed from  $10^4$  Monte Carlo simulation samples.

[Color figure can be viewed in the online issue, which is available at [wileyonlinelibrary.com](http://wileyonlinelibrary.com).]

desired species concentration with both a higher average and smaller standard deviation. In addition, parameterizing the dependence of the desired species concentration on the reaction temperature with the Legendre polynomials reduced the number of system evaluations required by optimization by a factor of 5.

For a continuous-flow tubular chemical reactor with five species, the residence time was optimized to maximize the concentration of a desired intermediate species in the presence of two uncertain kinetic parameters. This reactor design problem is also subject to a constraint that the remaining limiting reagent should be no greater than 1% of its starting amount. With similar distributions of the desired intermediate species concentrations from the nominal and the polynomial chaos-based optimal residence times, the polynomial chaos-based optimal residence time resulted in no constraint violations, whereas the nominal optimal residence time resulted in 18% constraint violation. Furthermore, design input parameterization reduced the number of system evaluations required by optimization by a factor of 17.

The design input parameterization significantly reduced the number of system evaluations required by optimization in both case studies. Also, including the effects of uncertainties in the optimal design problems via PCEs produced design inputs that simultaneously improved distribution of the optimization objective and increased the probability of constraint satisfaction.

PCEs are most effective when the objective and constraints are smooth functions of the uncertain parameters, which would be expected to occur in most chemical process design problems. When the objective and constraints are not smooth functions of the uncertain parameters, then accurate approxi-

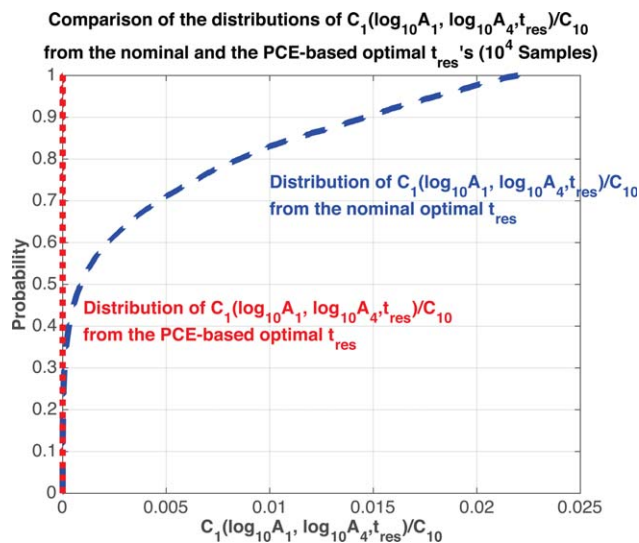


**Figure 7.** Comparison of the probability distribution functions of  $C_1(\log_{10} A_1, \log_{10} A_4, t_{res})/C_{10}$  from the nominal and the polynomial chaos-based optimal residence times for the tubular reactor case study, constructed from  $10^4$  Monte Carlo simulation samples.

[Color figure can be viewed in the online issue, which is available at [wileyonlinelibrary.com](http://wileyonlinelibrary.com).]

mation via PCEs will require a larger number of terms in the expansions and more system evaluations to compute the expansion coefficients, and efficient sampling methods can be less computationally expensive.<sup>24</sup> PCEs are also most effective when each objective or constraint is sensitive to a relatively small number of design inputs and uncertain parameters, e.g., less than ten. Properties of interest such as concentrations and yields for most chemical reaction networks and reaction-transport networks depend strongly on only a small number of key parameters, which are associated with rate-limiting steps.<sup>25</sup> A parameter sensitivity analysis can be conducted to determine which parameters in the design objective and each constraint to include in PCEs, while ignoring the parameters that have sufficiently low effects on the design objective and constraints. For process design problems that have larger numbers of sensitive uncertain parameters and/or design degrees of freedom, Smolyak sparse grids can be used to reduce the number of function evaluations required for PCE coefficient computation.<sup>22</sup>

Since the objective and constraints of the PCE-based optimization are represented by polynomials, the resulting optimizations are polynomial programs. Although this manuscript used local optimization, the polynomial dependencies mean that the optimization can be solved using any local or global optimization algorithms developed for the solution of polynomial programs.<sup>26,27</sup>

## Acknowledgment

Financial support from Novartis<sup>®</sup> is acknowledged.



## Literature Cited

1. Zang C, Friswell MI, Mottershead JE. A review of robust optimal design and its application in dynamics. *Comput Struct*. 2005;83:315–326.
2. Pistikopoulos EN. Uncertainty in process design and operations. *Comput Chem Eng*. 1995;19:553–563.
3. Grossmann IE, Sargent RWH. Optimum design of chemical plants with uncertain parameters. *AIChE J*. 1978;24:1021–1028.
4. Nagy ZK, Braatz RD. Distributional uncertainty analysis using power series and polynomial chaos expansions. *J Process Control* 2007;17:229–240.
5. Pishvae MS, Rabbani M, Torabi SA. A robust optimization approach to closed-loop supply chain network design under uncertainty. *Appl Math Model*. 2011;35:637–649.
6. Rustem B, Howe M. *Algorithms for Worst-Case Design and Applications to Risk Management*. Princeton, New Jersey: Princeton University Press, 2009.
7. Nagy ZK, Braatz RD. Open-loop and closed-loop robust optimal control of batch processes using distributional and worst-case analysis. *J Process Control* 2004;14:411–422.
8. Fisher J, Bhattacharya R. Linear quadratic regulation of systems with stochastic parameter uncertainties. *Automatica* 2009;45:2831–2841.
9. Mandur J, Budman H. Robust optimization of chemical processes using bayesian description of parametric uncertainty. *J Process Control* 2014;24:422–430.
10. Moon J, Kim S, Linninger AA. Integrated design and control under uncertainty: embedded control optimization for plantwide processes. *Comput Chem Eng*. 2011;35:1718–1724.
11. Wei J, Realff MJ. Sample average approximation methods for stochastic MINLPs. *Comput Chem Eng*. 2004;28:333–346.
12. Sahinidis NV. Optimization under uncertainty: state-of-the-art and opportunities. *Comput Chem Eng*. 2004;28:971–983.
13. Becker R, Hall SG, Rustem B. Robust optimal decisions with stochastic nonlinear economic systems. *J Econ Dynam Control* 1994; 18:125–147.
14. Iman RL, Conover WJ. Small sample sensitivity analysis techniques for computer models, with an application to risk assessment. *Commun Stat Theory Methods* 1980;9:1749–1842.
15. Diwekar UM, Kalagnanam JR. Efficient sampling technique for optimization under uncertainty. *AIChE J*. 1997;43:440–447.
16. Ierapetritou MG, Acevedo J, Pistikopoulos EN. An optimization approach for process engineering problems under uncertainty. *Comput Chem Eng*. 1996;20:703–709.
17. Xiu D, Karniadakis GE. The Wiener–Askey polynomial chaos for stochastic differential equations. *SIAM J Sci Comput*. 2002;24:619–644.
18. Babaei M, Alkhatib A, Pan I. Robust optimization of subsurface flow using polynomial chaos and response surface surrogates. *Comput Geosci*. 2015;19:979–998.
19. Hover FS, Triantafyllou MS. Application of polynomial chaos in stability and control. *Automatica* 2006;42:789–795.
20. İçten E, Nagy ZK, Reklaitis GV. Process control of a dropwise additive manufacturing system for pharmaceuticals using polynomial chaos expansion based surrogate model. *Comput Chem Eng*. 2015; 83:221–231.
21. Kim KKK, Shen DE, Nagy ZK, Braatz RD. Wiener’s polynomial chaos for the analysis and control of nonlinear dynamical systems with probabilistic uncertainties. *IEEE, Control Syst* 2013;33:58–67.
22. Eldred MS. Recent advances in non-intrusive polynomial chaos and stochastic collocation methods for uncertainty analysis and design. *AIAA Paper* 2009;2274:1–37.
23. Reizman BJ, Jensen KF. An automated continuous-flow platform for the estimation of multistep reaction kinetics. *Organ Process Res Dev*. 2012;16:1770–1782.
24. Crestaux T, Le Maître O, Martinez JM. Polynomial chaos expansion for sensitivity analysis. *Reliab Eng Syst Safe*. 2009;94:1161–1172.
25. Varma A, Morbidelli M, Wu H. *Parametric Sensitivity in Chemical Systems*. Cambridge, United Kingdom: Cambridge University Press, 2005.
26. Sahinidis NV. BARON: a general purpose global optimization software package. *J Glob Optim*. 1996;8:201–205.
27. Henrion D, Lasserre JB. GloptiPoly: global optimization over polynomials with matlab and SeDuMi. *ACM Trans Math Software* 2003; 29:165–194.

Manuscript received May 5, 2016, and revision received June 9, 2016.